Geology, published online on 24 January 2014 as doi:10.1130/G35073.1

Geology

Rift flank uplift at the Gulf of California: No requirement for asthenospheric upwelling

Chris Mark, Sanjeev Gupta, Andy Carter, Darren F. Mark, Cécile Gautheron and Arturo Martín

Geology published online 24 January 2014;
doi: 10.1130/G35073.1

Notes

Geology, published online on 24 January 2014 as doi:10.1130/G35073.1

Rift flank uplift at the Gulf of California: No requirement for asthenospheric upwelling

Chris Mark[1]*, Sanjeev Gupta[1], Andy Carter[2], Darren F. Mark[3], Cécile Gautheron[4], and Arturo Martín[5]
[1]Department of Earth Science and Engineering, South Kensington Campus, Imperial College London, London SW7 2AZ, UK
[2]Department of Earth and Planetary Sciences, Birkbeck, University of London, Malet Street, London WC1E 7HX, UK
[3]Natural Environment Research Council Argon Isotope Facility, Scottish Universities Environmental Research Centre, Rankine Avenue, Scottish Enterprise Technology Park, Glasgow G75 0QF, UK
[4]UMR Interaction et Dynamique des Environnements de Surface, CNRS 8148, Université Paris-Sud 11, 91405 Orsay, France
[5]Departamento de Geología, Centro de Investigación Científica y de Educación Superior de Ensenada, Carretera Ensenada-Tijuana 3918, 22860 Ensenada, Baja California, Mexico

ABSTRACT

Continental rifts are commonly flanked by zones of high elevation, but the cause of uplift remains controversial. Proposed uplift mechanisms include active and induced asthenospheric upwelling, and isostatically driven lithospheric flexure. Discrimination between these hypotheses requires close constraint of the timing of rift flank uplift and crustal extension. Here, we focus on the well-preserved Neogene Gulf of California rift. The western rift margin is characterized by a prominent east-facing kilometer-scale escarpment, which bounds a west-tilted, topographically asymmetric rift flank. We exploit west-draining canyons incised into the rift flank to constrain the timing of uplift to between ca. 5.6 and 3.2 Ma using ^{40}Ar/^{39}Ar dating of lavas, which show cut-and-fill relationships to the canyons. Rift flank uplift closely followed the onset of slip on the principal fault of the Loreto rift segment at ca. 8–6 Ma, the age of which we obtain from apatite (U-Th)/He and fission-track thermochronologic analysis of rift escarpment exhumation. Uplift was therefore coeval with lithospheric rupture and the onset of oceanic spreading between ca. 6 and 3 Ma, but post-dates a proposed asthenospheric upwelling event by ~8–10 Ma. The timing of uplift is inconsistent with either active or induced upwelling as uplift mechanisms, and we conclude that rift flank uplift was driven by the flexural response to lithospheric unloading.

INTRODUCTION

The observation that many rifts are bounded by elevated flanks raises the question of how high topography is generated at zones of crustal thinning. Many have recognized that the key to this problem lies in the timing of uplift and crustal extension. Surface uplift prior to extension indicates active asthenospheric upwelling as the driving mechanism, because upwelling should cause topographic doming (Cox, 1989; Ziegler and Cloetingh, 2004). Conversely, synchronous uplift and rifting implicate the flexurally distributed isostatic response to lithospheric unloading (Braun and Beaumont, 1989; Weissel and Karner, 1989) or induced asthenospheric convection (Buck, 1986; Huismans et al., 2001) as the uplift mechanisms. Therefore, establishing the timing of rift flank surface uplift and crustal extension allows identification of the rift flank uplift mechanism.

The Gulf of California is an oblique transtensional rift which has accommodated divergent motion of the Pacific and North America plates subsequent to foundering of the oceanic Farallon plate beneath North America. Subduction slowed and ceased between ca. 15 and 11.5 Ma (Lonsdale, 1991; Tian et al., 2011); major crustal thinning began no earlier than ca. 9 Ma (Oskin and Stock, 2003; Seiler et al., 2011), and progressed to lithospheric rupture and the onset of seafloor spreading at ca. 6–3 Ma (Lonsdale, 1991; Lizarralde et al., 2007). Although rift development has been closely linked to the plate boundary reorganization, a prominent role has also been proposed for active asthenospheric upwelling through a slab window opened by slab tear as subduction ceased (Fletcher et al., 2007). Compositional analyses of synrift lavas to confirm asthenospheric upwelling have proved inconclusive (Negrete-Aranda and Cañón-Tapia, 2008; Calmus et al., 2011). However, numerical modeling of slab detachment indicates that any topographic response should occur within <2 Ma of upwelling (Duretz et al., 2011). As slab window opening pre-dates rifting, establishing the timing of rift flank surface uplift and crustal extension allows a test of the hypothesis that rift flank uplift was driven by pre-rift asthenospheric upwelling.

GEOLOGICAL AND GEOMORPHIC SETTING

We focus on the Loreto rift segment of the Baja California Peninsula (Umhoefer et al., 2002). Here, the east-facing escarpment separates a low-elevation coastal plain, which hosts the rift-bounding, east-dipping Loreto segment faults and a Pliocene rift basin (Dorsey and Umhoefer, 2000), from a west-sloping rift flank (Fig. 1). The oldest dateable unit in the rift basin was deposited at ca. 2.6 Ma, but the age of deposition onset is unknown (Dorsey and Umhoefer, 2000). The regional geology comprises pre-Cretaceous metasediments and Cretaceous granodiorite basement, overlain by the ~1–1.5-km-thick volcaniclastic Comondú Group, a remnant of the former subduction arc (Umhoefer et al., 2001). The Comondú Group is discontinuously overlain on the rift flank by widespread post-subduction transitional and alkalic lavas (Sawlan, 1991; Calmus et al., 2011). The escarpment crest forms the regional drainage divide, attaining elevations here of ~1–1.6 km above sea level (asl), and is offset from the Loreto fault by a ~3–5-km-wide, low-elevation eroded piedmont, exposing the basement (Fig. 1). The piedmont was formed by westward retreat of the escarpment from the fault, and we investigate this piedmont denudation using the apatite fission track (AFT) and apatite (U-Th)/He (AHe) thermochronometers. These are sensitive to cooling over the range ~120–40 °C, and are widely used to detect episodes of burial and exhumation affecting shallow crustal levels (Gallagher et al., 1998; Farley, 2000). As piedmont exhumation and escarpment development were driven by Loreto fault slip, cooling ages provide a proxy for the local timing of crustal extension.

West of the escarpment crest, the rift flank is incised by a network of west-draining canyons, attaining typical depths of ~400–600 m at the escarpment crest, which commonly beheads them (Fig. 1A). The canyon network therefore extended east of the modern divide at the escarpment crest, either to the crest of a paleo-escarpment formed at the Loreto fault after rifting but prior to escarpment retreat, or further east to a pre-rift drainage divide. Incision therefore occurred before or after the onset of crustal extension. Fluvial incision is a commonly used proxy for surface uplift (Schildgen et al., 2007); canyon incision depths provide the minimum uplift magnitude. Crucially, the canyons transect the post-subduction lavas of the rift flank, allowing us to construct a detailed ^{40}Ar/^{39}Ar chronology of rift flank canyon incision as a proxy for the timing of surface uplift.

*Current address: Department of Geology, School of Natural Sciences, Trinity College Dublin, Dublin 2, Ireland; E-mail: markc@tcd.ie.

Data Repository item 2014102 | doi:10.1130/G35073.1

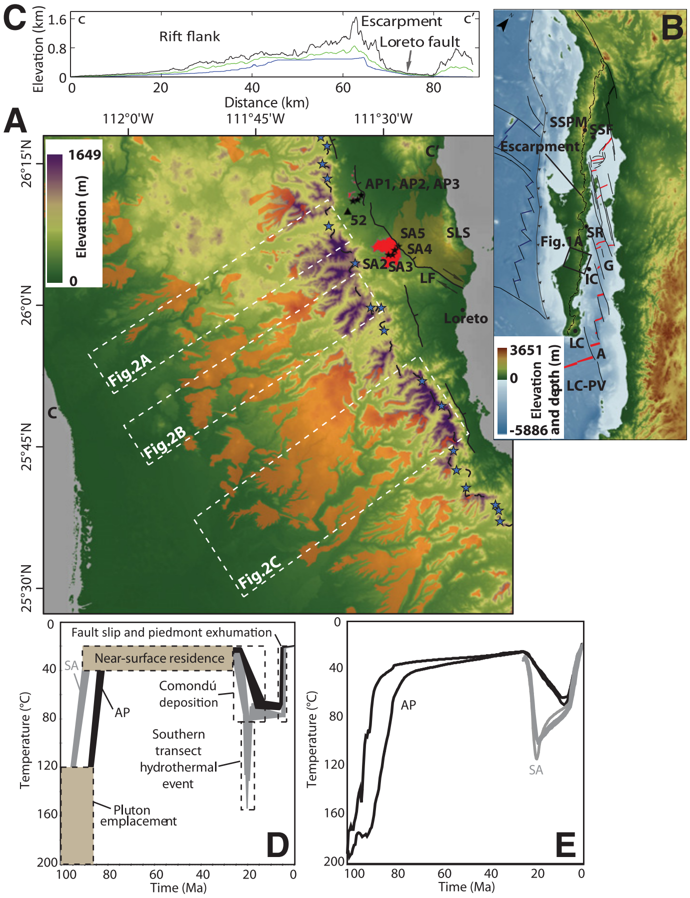

Figure 1. Gulf of California and Loreto rift segment. A: Topography of Loreto rift segment, showing Loreto segment faults (black), relict landscape (orange overlay), Loreto basin (brown) east of Loreto fault, piedmont granodiorite exposures (red), beheaded canyons (blue stars), piedmont lava sample site (black triangle), piedmont granodiorite sample sites (black stars), and escarpment crest (black dashed line). SLS—Sierra La Sierrita; LF—Loreto fault. B: Topography of Gulf of California, showing principal transfer zones (black), active spreading centers of the gulf (red), and Pacific-Farallon fossil spreading centers (blue). SSF—Sierra San Felipe; SSPM—Sierra San Pedro Mártir; SR—Santa Rosalía; IC—Isla Carmen; LC—Los Cabos; G—Guaymas spreading center; A—Alarcón center; LC-PV—Los Cabos–Puerto Vallarta center. C: Maximum (black), mean (green), and minimum (blue) topography along 5-km-wide swath across the peninsula. D: Summary of acceptable thermal histories of northern (AP) and southern (SA) transect piedmont basement samples, derived from forward modeling. E: Weighted mean paths of acceptable thermal histories derived from inverse modeling. Thermal histories of southern transect samples are unconstrained prior to ca. 25 Ma but were likely similar to those of northern transect.

TIMING OF CRUSTAL EXTENSION AT LORETO

Results of the AHe and AFT Analyses

We collected granodiorite basement samples from the piedmont along two transects perpendicular to the escarpment, between ~100 and 200 m asl. Southern transect mean AHe ages range from 4.8 ± 0.6 Ma to 5.1 ± 0.3 Ma; northern ages are slightly older, at 6.5 ± 0.4 Ma to 7.6 ± 0.6 Ma. Southern and northern AFT ages are 17.0 ± 1.8 Ma to 25.1 ± 2.6 Ma, and 79.3 ± 2.5 Ma to 84.0 ± 3.0 Ma, respectively. Zircon U-Pb ages obtained from one sample from each transect yielded pluton emplacement ages of 91.0 ± 0.5 Ma and 100.3 ± 0.8 Ma, respectively. Data here and throughout are reported at the 1σ confidence level (Fig. 1; Tables DR1–DR4 and Fig. DR1 in the GSA Data Repository[1]).

Thermal History Modeling

To reconcile the discrepancy between the northern and southern transect AFT and AHe ages, we carried out thermal history modeling using the HeFTy program of Ketcham (2005) with standard annealing and He diffusion kinetics (Ketcham et al., 1999; Farley, 2000; see the Data Repository). For all samples, acceptable time-temperature paths require rapid cooling from peak temperatures of ~60–80 °C to <50 °C between ca. 8 and 3 Ma (Figs. 1D and 1E; Fig. DR2). The older AHe ages of the northern transect can be explained by rapid post-emplacement cooling and continuous residence at temperatures <90 °C since the late Cretaceous, as required by late Cretaceous AFT ages. Partial retention of He accumulated since this time would generate the older AHe ages. Southern transect samples experienced cooling from >120 °C in the early Miocene (Figs. 1D and 1E), coincident with deposition of the lowermost units of the overlying Comondú Group, prohibiting cooling by exhumation. Instead, the presence of epidote alteration and disseminated malachite indicates localized hydrothermal processes were responsible, perhaps linked to early Comondú volcanism.

We interpret the cooling experienced by all samples between ca. 8 and 3 Ma as erosional exhumation of the piedmont driven by Loreto fault slip. This interpretation is also consistent with an $^{40}Ar/^{39}Ar$ age of 5.655 ± 0.152 Ma obtained from an isolated post-subduction lava flow overlying the piedmont ~4.5 km west of the Loreto fault, which therefore constrains the onset of exhumation to ca. 8–6 Ma (Fig. 1; Table DR5; Figs. DR7 and DR8). Estimated peak burial temperatures of ~60–80 °C (Figs. 1D and 1E; Fig. DR2) match exhumation depths of ~1.4–2 km (Fig. 1C), assuming a surface temperature of 20 °C and geothermal gradients of ~20–43 °C km^{-1}, consistent with values reported elsewhere in the gulf (Fletcher et al., 2000; Seiler et al., 2011). A significant lag between fault slip and piedmont exhumation onset is excluded, as the samples closest to the fault (AP3 and SA5) do not yield older ages than samples further west. Equally, exhumation cannot have been driven by westward retreat of an escarpment formed at an older fault offshore prior to Loreto fault initiation, as this would have removed upper Comondú volcanics exposed in the Sierra La Sierrita in the Loreto fault hanging wall (Umhoefer et al., 2001). Crustal extension at Loreto therefore began between ca. 8 and 6 Ma, similar to the post–8 Ma onset at the Santa Rosalía Basin, (Conly et al., 2005), the ca. 8–4 Ma onset at Isla Carmen (Dorsey et al., 2001), the ca. 9–7 Ma onset at the Sierra San Felipe (Seiler et al., 2011), and the ca. 12–7 Ma onset at Los Cabos (Fletcher et al., 2000).

TIMING OF RIFT FLANK SURFACE UPLIFT

To constrain the timing of surface uplift, we investigated the development of the west-draining rift flank canyons. We discount climate change as a cause of canyon incision, as analysis of paleosols and offshore sediment palynology in the northern gulf indicate a stable regional climate during the late Miocene to mid-Pliocene (Ballog and Malloy, 1981; Peryam et al., 2011). Between the canyons, the summits of the interfluve mesas preserve a westward-sloping, low-relief relict landscape (Figs. 1A, 2, and 3). This landscape developed atop the Comondú Group (Fig. DR3), and is characterized by discontinuous deposits of poorly consolidated alluvial cobbles up to ~30 m thick. Cobble lithologies indicate sourcing primarily from post-subduction and upper Comondú lavas, indicating that they are not reworked from lower Comondú conglomerates (Fig. DR4). Mesa-top alluvial deposits interfinger with post-subduction lava flows incised by the rift flank canyons. Preservation of these surficial features indicates that the low-relief mesa-top summits preserve the pre-incision low-relief landscape. These incised relict landscape lavas therefore provide a maximum

[1]GSA Data Repository item 2014102, details and tabulated full results of thermochronologic and Ar isotope analyses, is available online at www.geosociety.org/pubs/ft2014.htm, or on request from editing@geosociety.org or Documents Secretary, GSA, P.O. Box 9140, Boulder, CO 80301, USA.

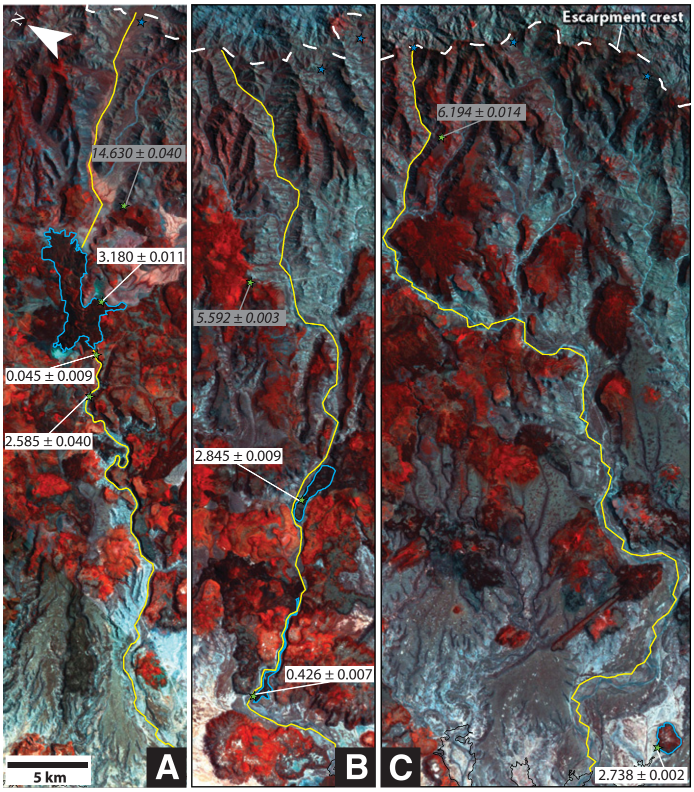

Figure 2. Rift flank canyons and sample locations. Multi-band LANDSAT false color composite (band combination BGR127). See Figure 1 for canyon locations. A: Comondú canyon. B: San Venancio canyon. C: San Javier canyon. Post-subduction lavas are red; mesa-capping relict landscape alluvial deposits are gray. Sampled canyon-filling lavas outlined in blue, and streams shown in yellow. Lava sample locations shown by green stars; $^{40}Ar/^{39}Ar$ ages in Ma. Incised relict landscape lava ages in italics; canyon-filling lava ages in regular text.

age for incision onset. Samples obtained from these lavas yield $^{40}Ar/^{39}Ar$ ages of 14.630 ± 0.040 Ma to 5.592 ± 0.003 Ma, indicating that the low-relief relict landscape developed during this time, prior to canyon incision (Fig. 2; Table DR5; Figs. DR5, DR7, and DR8).

Lavas that flowed into canyons after the onset of incision provide minimum ages for incision to the depth of each lava flow (Fig. 2; Table DR5; Figs. DR6–DR8; see the Data Repository for descriptions). These lavas yield $^{40}Ar/^{39}Ar$ ages of 3.180 ± 0.011 Ma to 0.045 ± 0.009 Ma. These data therefore constrain the bulk of rift flank canyon incision, our surface uplift proxy, to between ca. 5.6 and 3.2 Ma.

DISCUSSION

Rift flank uplift was thus coeval with, or shortly post-dated, the major period of active faulting and escarpment development at Loreto between ca. 8 and 6 Ma. Uplift occurred ~8–10 Ma after slab window opening beneath the gulf, inferred from the abandoned Pacific-Farallon spreading centers preserved offshore southern Baja California (Lonsdale, 1991). Seafloor magnetic anomalies indicate these rotated clockwise 45°–60° between ca. 15 and 14 Ma, likely due to a loss of slab pull (Bohannon and Parsons, 1995; Tian et al., 2011). Slab tear does coincide with ongoing extension east of the gulf, which is spatially and temporally contiguous with older extension of the southern Basin and Range province, but this region has undergone Neogene topographic collapse, not uplift (Ferrari et al., 2013). Regional pre-rift topographic doming therefore did not occur, and we conclude that no precursor asthenospheric upwelling occurred beneath the southern gulf in the late Miocene.

The timing of uplift does overlap with lithospheric rupture and the onset of oceanic spreading at the Guaymas, Alarcón, and Cabo–Puerto Vallarta centers between ca. 6 and 3 Ma (Lizarralde et al., 2007). We propose that rift flank uplift was driven by the flexurally distributed isostatic response to crustal unloading associated with lithospheric rupture. Two-dimensional modeling of the flexural response to unloading can replicate the observed uplift magnitude and wavelength (see Figs. 3D–3F, Fig. DR9, and the Data Repository). We exclude any contribution from small-scale induced asthenospheric convection (Buck, 1986) because surface wave tomography suggests convection is not occurring beneath the southern gulf,

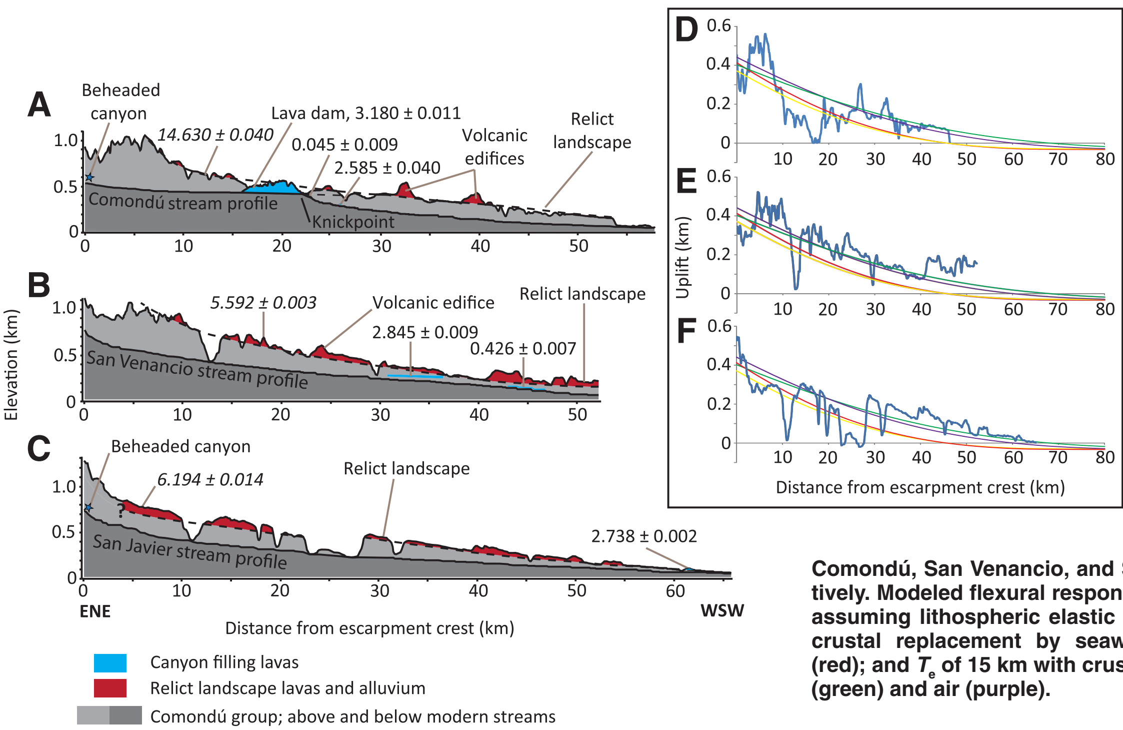

Figure 3. A–C: Stream profiles from escarpment crest to 50 m contour for Comondú (A), San Venancio (B), and San Javier (C) canyons (see Fig. 2 for locations). Upper profile on each plot shows interfluve elevations; dashed black line shows top of Comondú Group units. Overlying relict landscape alluvial deposits and lava flows in red; canyon-filling lavas in blue. $^{40}Ar/^{39}Ar$ ages in Ma; incised lava ages in italics; canyon-filling lava ages in regular text. D–F: Minimum uplift magnitudes (interfluve elevation minus stream elevation; blue line) for Comondú, San Venancio, and San Javier canyons, respectively. Modeled flexural responses to unloading are shown, assuming lithospheric elastic thickness (T_e) of 10 km and crustal replacement by seawater (yellow) and air infill (red); and T_e of 15 km with crustal replacement by seawater (green) and air (purple).

as fragments of the Farallon slab stalled beneath Baja California inhibit return flow (Zhang and Paulssen, 2012). Induced convective upwelling may be responsible for the higher elevation of the rift flank in the north of the gulf where stalled fragments are absent (Zhang and Paulssen, 2012); however, O'Connor and Chase (1989) show that the observed topography of the Sierra San Pedro Mártir can also be explained by flexural uplift during rifting driven by release of a previously suppressed crustal root.

In summary, we have shown that the flexural isostatic response to crustal unloading is a viable mechanism of rift flank uplift, as proposed by Braun and Beaumont (1989) and Weissel and Karner (1989); asthenospheric upwelling need not be invoked. It is striking that the complex asthenospheric history of subduction, slab tear, and window formation appears to have had little influence on the topographic development of the Gulf of California rift.

ACKNOWLEDGMENTS

C. Mark was supported by NERC doctoral training grant NE/G523547/1; Ar isotope work was supported by NERC AIF grant IP-1153-1109 made to S. Gupta; AHe analysis was supported by ANR grant ANR-06-JCJC-0079 made to C. Gautheron; and fieldwork was in part funded by a Santander International Mobility Award to C. Mark. We thank M. Cruickshanks and T. Horner for field assistance; J. Imlach and R. Dymock (SUERC) for assistance with ^{40}Ar/^{39}Ar analysis; R. Pinna (UMR IDES) for assistance with AHe analysis; and A. Densmore for providing the swath profile tool. P. Allen, B. Coakley, and S. Goes are thanked for helpful discussion, and also G. Axen, M. Oskin, and an anonymous reviewer for comments that greatly improved the manuscript.

REFERENCES CITED

Ballog, R.A., and Malloy, R.E., 1981, Neogene palynology from the southern California continental borderland, Site 467, Deep Sea Drilling Project Leg 63, *in* Yeats, R.S., Haq, B.U., et al., Initial Reports of the Deep Sea Drilling Project, Volume 63: Washington, D.C., U.S. Government Printing Office, p. 565–576, doi:10.2973/dsdp.proc.63.116.1981.

Bohannon, R.G., and Parsons, T., 1995, Tectonic implications of post–30 Ma Pacific and North American relative plate motions: Geological Society of America Bulletin, v. 107, p. 937–959, doi:10.1130/0016-7606(1995)107<0937:TIOPMP>2.3.CO;2.

Braun, J., and Beaumont, C., 1989, A physical explanation of the relation between flank uplifts and the breakup unconformity at rifted continental margins: Geology, v. 17, p. 760–764, doi:10.1130/0091-7613(1989)017<0760:APEOTR>2.3.CO;2.

Buck, W.R., 1986, Small-scale convection induced by passive rifting: The cause for uplift of rift shoulders: Earth and Planetary Science Letters, v. 77, p. 362–372, doi:10.1016/0012-821X(86)90146-9.

Calmus, T., Pallares, C., Maury, R.C., Aguillón-Robles, A., Bellon, H., Benoit, M., and Michaud, F., 2011, Volcanic markers of the post-subduction evolution of Baja California and Sonora, Mexico: Slab tearing versus lithospheric rupture of the Gulf of California: Pure and Applied Geophysics, v. 168, p. 1303–1330, doi:10.1007/s00024-010-0204-z.

Conly, A.G., Brenan, J.M., and Scott, S.D., 2005, Arc to rift transitional volcanism in the Santa Rosalía Region, Baja California Sur, Mexico: Journal of Volcanology and Geothermal Research, v. 142, p. 303–341, doi:10.1016/j.jvolgeores.2004.11.013.

Cox, K., 1989, The role of mantle plumes in the development of continental drainage patterns: Nature, v. 342, p. 873–877, doi:10.1038/342873a0.

Dorsey, R.J., and Umhoefer, P.J., 2000, Tectonic and eustatic controls on sequence stratigraphy of the Pliocene Loreto basin, Baja California Sur, Mexico: Geological Society of America Bulletin, v. 112, p. 177–199, doi:10.1130/0016-7606(2000)112<177:TAECOS>2.0.CO;2.

Dorsey, R.J., Umhoefer, P.J., Ingle, J.C., and Mayer, L., 2001, Late Miocene to Pliocene stratigraphic evolution of northeast Carmen Island, Gulf of California: Implications for oblique-rifting tectonics: Sedimentary Geology, v. 144, p. 97–123, doi:10.1016/S0037-0738(01)00137-3.

Duretz, T., Gerya, T.V., and May, D.A., 2011, Numerical modeling of spontaneous slab breakoff and subsequent topographic response: Tectonophysics, v. 502, p. 244–256, doi:10.1016/j.tecto.2010.05.024.

Farley, K.A., 2000, Helium diffusion from apatite: General behavior as illustrated by Durango fluorapatite: Journal of Geological Research, v. 105, p. 2903–2914, doi:10.1029/1999JB900348.

Ferrari, L., López-Martínez, M., Orozco-Esquivel, T., Bryan, S.E., Duque-Trujillo, J., Lonsdale, P., and Solari, L., 2013, Late Oligocene to Middle Miocene rifting and synextensional magmatism in the southwestern Sierra Madre Occidental, Mexico: The beginning of the Gulf of California rift: Geosphere, v. 9, p. 1161–1200, doi:10.1130/GES00925.1.

Fletcher, J.M., Kohn, B.P., Foster, D.A., and Gleadow, A.J.W., 2000, Heterogeneous Neogene cooling and exhumation of the Los Cabos block, southern Baja California: Evidence from fission-track thermochronology: Geology, v. 28, p. 107–110, doi:10.1130/0091-7613(2000)28<107:HNCAEO>2.0.CO;2.

Fletcher, J.M., Grove, M., Kimbrough, D., Lovera, O., and Gehrels, G.E., 2007, Ridge-trench interactions and the Neogene tectonic evolution of the Magdalena shelf and southern Gulf of California: Insights from detrital zircon U-Pb ages from the Magdalena fan and adjacent areas: Geological Society of America Bulletin, v. 119, p. 1313–1336, doi:10.1130/B26067.1.

Gallagher, K., Brown, R.W., and Johnson, C., 1998, Fission track analysis and its applications to geological problems: Annual Review of Earth and Planetary Sciences, v. 26, p. 519–572, doi:10.1146/annurev.earth.26.1.519.

Huismans, R., Podladchikov, Y.Y., and Cloetingh, S., 2001, Transition from passive to active rifting: Relative importance of asthenospheric doming and passive extension of the lithosphere: Journal of Geophysical Research, v. 106, p. 11,271–11,291, doi:10.1029/2000JB900424.

Ketcham, R.A., 2005, Forward and inverse modeling of low-temperature thermochronometry data, *in* Reiners, P.W., and Ehlers, T.A., eds., Low-temperature thermochronology: Techniques, interpretations, and applications: Mineralogical Society of America Reviews in Mineralogy and Geochemistry, v. 58, p. 275–314.

Ketcham, R.A., Donelick, R.A., and Carlson, W.D., 1999, Variability of apatite fission-track annealing kinetics III: Extrapolation to geological time scales: The American Mineralogist, v. 84, p. 1235–1255.

Lizarralde, D., Axen, G.J., Brown, H.E., Fletcher, J.M., Gonza, A., Harding, A.J., Holbrook, W.S., Kent, G.M., Paramo, P., Sutherland, F., and Umhoefer, P.J., 2007, Variation in styles of rifting in the Gulf of California: Nature, v. 448, p. 466–469, doi:10.1038/nature06035.

Lonsdale, P.F., 1991, Structural patterns of the Pacific floor offshore of Peninsular California, *in* Dauphin, J.P., and Simoneit, R.T., eds., The Gulf and Peninsular Province of the Californias: American Association of Petroleum Geologists Memoir 47, p. 87–125.

Negrete-Aranda, R., and Cañón-Tapia, E., 2008, Post-subduction volcanism in the Baja California Peninsula, Mexico: The effects of tectonic reconfiguration in volcanic systems: Lithos, v. 102, p. 392–414, doi:10.1016/j.lithos.2007.08.013.

O'Connor, J., and Chase, C., 1989, Uplift of the Sierra San Pedro Mártir, Baja California, Mexico: Tectonics, v. 8, p. 833–844, doi:10.1029/TC008i004p00833.

Oskin, M., and Stock, J., 2003, Marine incursion synchronous with plate-boundary localization in the Gulf of California: Geology, v. 31, p. 23–26, doi:10.1130/0091-7613(2003)031<0023.

Peryam, T.C., Dorsey, R.J., and Bindeman, I., 2011, Plio-Pleistocene climate change and timing of Peninsular Ranges uplift in southern California: Evidence from paleosols and stable isotopes in the Fish Creek–Vallecito basin: Palaeogeography, Palaeoclimatology, Palaeoecology, v. 305, p. 65–74, doi:10.1016/j.palaeo.2011.02.014.

Sawlan, M.G., 1991, Magmatic evolution of the Gulf of California rift, *in* Dauphin, J., and Simoneit, B., eds., The Gulf and Peninsular Province of the Californias: American Association of Petroleum Geologists Memoir 47, p. 301–369.

Schildgen, T.F., Hodges, K.V., Whipple, K.X, Reiners, P.W., and Pringle, M.S., 2007, Uplift of the western margin of the Andean plateau revealed from canyon incision history, southern Peru: Geology, v. 35, p. 523–526, doi:10.1130/G23532A.1.

Seiler, C., Fletcher, J.M., Kohn, B.P., and Gleadow, A.J.W., 2011, Low-temperature thermochronology of northern Baja California, Mexico: Decoupled slip-exhumation gradients and delayed onset of oblique rifting across the Gulf of California: Tectonics, v. 30, TC3004, doi:10.1029/2009TC002649.

Tian, L., Castillo, P.R., Lonsdale, P.F., Hahm, D., and Hilton, D.R., 2011, Petrology and Sr-Nd-Pb-He isotope geochemistry of postspreading lavas on fossil spreading axes off Baja California Sur, Mexico: Geochemistry Geophysics Geosystems, v. 12, Q0AC10, doi:10.1029/2010GC003319.

Umhoefer, P.J., Dorsey, R.J., Willsey, S., Mayer, L., and Renne, P., 2001, Stratigraphy and geochronology of the Comondú Group near Loreto, Baja California Sur, Mexico: Sedimentary Geology, v. 144, p. 125–147, doi:10.1016/S0037-0738(01)00138-5.

Umhoefer, P.J., Mayer, L., and Dorsey, R.J., 2002, Evolution of the margin of the Gulf of California near Loreto, Baja California Peninsula, Mexico: Geological Society of America Bulletin, v. 114, p. 849–868, doi:10.1130/0016-7606(2002)114<0849:EOTMOT>2.0.CO;2.

Weissel, J.K., and Karner, G.D., 1989, Flexural uplift of rift flanks due to mechanical unloading of the lithosphere during extension: Journal of Geophysical Research, v. 94, p. 13,919–13,950, doi:10.1029/JB094iB10p13919.

Zhang, X., and Paulssen, H., 2012, Geodynamics of the Gulf of California from surface wave tomography: Physics of the Earth and Planetary Interiors, v. 192–193, p. 59–67, doi:10.1016/j.pepi.2011.12.001.

Ziegler, P.A., and Cloetingh, S., 2004, Dynamic processes controlling evolution of rifted basins: Earth-Science Reviews, v. 64, p. 1–50, doi:10.1016/S0012-8252(03)00041-2.

Manuscript received 29 August 2013
Revised manuscript received 4 December 2013
Manuscript accepted 11 December 2013

Printed in USA